Molecular Pharmacology Fast Forward. Published on April 23, 2009 as doi:10.1124/mol.108.053751

In vivo and *in vitro* structure-activity relationships and structural conformation of kisspeptin-10-related peptides

Ester Gutiérrez-Pascual, Jérôme Leprince, Antonio J. Martínez-Fuentes, Isabelle Ségalas-Milazzo, Rafael Pineda, Juan Roa, Mario Duran-Prado, Laure Guilhaudis, Elia Desperrois, Aurélie Lebreton, Leonor Pinilla, Marie-Christine Tonon, María M. Malagón, Hubert Vaudry, Manuel Tena-Sempere, Justo P. Castaño

Department of Cell Biology, Physiology and Immunology, University of Córdoba, and CIBER Fisiopatología de la Obesidad y Nutrición (CIBERobn 06/03), Córdoba, Spain, EGP, AJMF, RP, JR, MDP, LP, MMM, MTS, JPC

Laboratory of Cellular and Molecular Neuroendocrinology, Inserm U413, UA CNRS, EA 4310, International Associated Laboratory Samuel de Champlain, European Institute for Peptide Research (IFRMP23), University of Rouen, Regional Platform for Cell Imaging (PRIMACEN), Mont-Saint-Aignan, France, JL, MT,HV.

Laboratory of Nuclear Magnetic Resonance, CNRS UMR 6014, IFRMP23, University of Rouen, Mont-Saint-Aignan, France, ISM, LG, ED, AL.

Molecular Pharmacology Fast Forward. Published on April 23, 2009 as DOI: 10.1124/mol.108.053751
This article has not been copyedited and formatted. The final version may differ from this version.

Running title: Structure-activity evaluation of kisspeptin analogs

Corresponding author: Dr. Justo P. Castaño
Department of Cell Biology, Physiology and Immunology
Edificio Severo Ochoa. Planta 3. Campus de Rabanales.
University of Córdoba
E-14014 Córdoba
Spain.
E-mail: justo@uco.es

Document statistics :

Number of text pages: 21

Number of tables: 2

Number of figures: 6

Number of words in Abstract: 351

Number of words in Introduction: 1040

Number of words in Discussion: 1389

List of non-standard abbreviations :

Kisspeptin-10 (Kp-10), luteinizing hormone (LH), free cytosolic calcium concentration ([Ca2+]i), orchidectomized (ORX).

Molecular Pharmacology Fast Forward. Published on April 23, 2009 as DOI: 10.1124/mol.108.053751
This article has not been copyedited and formatted. The final version may differ from this version.

ABSTRACT

Kisspeptins, the natural ligands of the G protein-coupled receptor KISS1R, comprise a family of related peptides derived from the proteolytic processing of a common precursor encoded by the *KISS1* gene. Among those, Kisspeptin-10 (Kp-10) contains the basic residues to retain full functional activity, and exhibits higher receptor affinity and biopotency than longer forms of the peptide. Although kisspeptins were first characterized by their ability to inhibit tumor metastasis, recent studies have revealed that the KISS1/KISS1R system plays an essential role in the neuroendocrine control of the reproductive axis. In this context, development and functional analysis of Kp-10 analogs may help searching new agonists and antagonists, as valuable tools to manipulate the KISS1/KISS1R system and, hence, fertility. We report herein functional and structural analyses of a series of Ala-substituted rat kp-10 analogs, involving $[Ca^{2+}]_i$ responses in rat kiss1r-transfected CHO cells, dynamic LH responses *in vivo,* and NMR structural studies. *In vitro* assays revealed that Ala-substitutions in positions 6 or 10 of kp-10 resulted in a significant increase in EC_{50} values (> $6.46x10^{-6}$M vs. 1.54–$2.6x10^{-8}$M for rat and human Kp-10), and a substantial decrease in the proportion of responsive cells coupled to a marked increase in the time required to reach maximal response. *In vivo* assays showed that Ala^6 substitution diminished, and Ala^{10} substitution eliminated, LH secretory responses, whereas co-administration of each analog failed to affect the LH-releasing ability of kp-10. Molecular modeling under NMR restraints revealed that kp-10 exhibits a helicoidal structure between the Asn^4 and Tyr^{10} residues, with mixed α- and 3_{10} characteristics. Ala^6 substitution induced limited destabilization of the helix around the position of the substitution. Ala^{10} substitution was found to totally disrupt the helical structure in the C-terminal region of the molecule. Taken together, our results indicate that positions 6 and 10 are critical for kp-10 action at kiss1r, and suggest that modifications in these positions could lead to the generation of new kisspeptin agonists and/or antagonists with altered functional and perhaps binding properties. Further, they emphasize the importance of using combined, multidisciplinary approaches, including *in vivo* studies, to reliably evaluate structure function properties of novel kisspeptin analogs.

Molecular Pharmacology Fast Forward. Published on April 23, 2009 as DOI: 10.1124/mol.108.053751
This article has not been copyedited and formatted. The final version may differ from this version.

Introduction

The ligand-receptor tandem comprised by kisspeptins and kiss1r has been the focus of intense research over the last decade owing to its peculiar dual pathophysiological relevance. *KISS1* gene was initially discovered in 1996 as a tumor suppressor gene, and was subsequently found to inhibit metastasis in melanoma and breast cancer cells (Lee et al., 1996; Lee and Welch, 1997). Five years later, three different groups identified kiss1r as the receptor for the family of peptides derived by proteolytic processing of a precursor protein encoded by *kiss1*, the kisspeptins, and characterized the basic pharmacological, signaling and functional properties of the kisspeptin/kiss1r system (Kotani et al., 2001; Muir et al., 2001; Ohtaki et al., 2001). These studies also showed that KISS1 is widely produced throughout the central nervous system and other organs, such as liver, lung, gonads and prostate (Muir et al., 2001, Ohtaki et al., 2001). A series of subsequent reports added convincing evidence indicating that this system was able to counteract metastasis, cell migration and proliferation in different cancer cell models, and established the presence and potential pathological relevance of kisspeptins and kiss1r in different types of cancers (Mead et al., 2007; Nash and Welch, 2006).

On a completely different scenario, two independent groups identified in late 2003 mutations in *KISS1R* as the underlying cause of hypogonadotropic hypogonadism in humans (de Roux et al., 2003; Seminara et al., 2003). This finding, coupled to the ensuing demonstration that lack of *kiss1r* (Funes et al., 2003; Seminara et al., 2003) and, more recently, *kiss1* (d'Anglemont de Tassigny et al., 2007; Lapatto et al., 2007) gene caused an identical reproductive disruption phenotype in mouse, paved the way for the unexpected establishment of kisspeptin/kiss1r as a novel, critical component for the control of the reproductive axis (Popa et al., 2008; Roa et al., 2008). In fact, there is now growing evidence that hypothalamic kiss1 and kiss1r act as key integrative players in the hierarchical control of reproduction, mainly by conveying to

Molecular Pharmacology Fast Forward. Published on April 23, 2009 as DOI: 10.1124/mol.108.053751
This article has not been copyedited and formatted. The final version may differ from this version.

the neurons releasing GnRH the central and peripheral signals that regulate (at least) puberty onset, ovulation, and sensing of metabolic status (Popa et al., 2008; Roa et al., 2008).

Despite the obvious interest raised by the potential pathophysiological implications of kisspeptins and kiss1r, relatively few studies have been addressed to date at elucidating in detail the structural and molecular features of this tandem, their pharmacology and related signal transduction pathways (Castaño et al., 2008). In particular, only a limited number of reports have analyzed the structure-activity relationships of kisspeptins and kiss1r (Niida et al., 2006; Orsini et al., 2007; Tomita et al., 2007a; Tomita et al., 2006; Tomita et al., 2007b; Tomita et al., 2008) and none has integrated the chemical structure of this peptide family, its functional features in cell models *in vitro*, and its effects *in vivo* in a physiologically relevant target.

Proteolytic processing of the precursor encoded by the *kiss1* gene predominantly generates Kisspeptin-54, also known as metastin, as well as lower amounts of shorter peptide fragments, including Kisspeptin-14, Kisspeptin-13 and Kisspeptin-10 (Mead et al., 2007; Nash and Welch, 2006; Popa et al., 2008; Roa et al., 2008). Earlier reports showed that kisspeptins share the 10-amino acid C-terminal region (H-Tyr-Asn-Trp-Asn-Ser-Phe-Gly-Leu-Arg-Phe-NH_2), which contains the canonical Arg-Phe-NH_2 motif of the RFamide peptide family. This structure is highly conserved across species, since in rat, mouse, ornithorhyncus, sheep and cow, Kp-10 only differs by one amino acid from the sequence of human and non-human primates (a C-terminal Tyr instead of Phe) (Roa and Tena-Sempere, 2007). Functional studies indicated that all kisspeptins are highly potent in terms of receptor activation, with shorter forms being even more active than Kisspeptin-54 (Kotani et al., 2001; Muir et al., 2001; Ohtaki et al., 2001). Using different cell lines expressing kiss1r, it has been established that coupling of kisspeptins to this receptor induces, as its major signaling cascade, activation of phospholipase C and polyphosphoinositide (PIP_2) hydrolysis,

Molecular Pharmacology Fast Forward. Published on April 23, 2009 as DOI: 10.1124/mol.108.053751
This article has not been copyedited and formatted. The final version may differ from this version.

followed by accumulation of inositol-(1,4,5)-triphosphate, Ca^{2+} mobilization, as well as phosphorylation of ERK1/2 and p38 MAP kinases (Castaño et al., 2008). In support of this, we have shown that, in rat hypothalamic explants, kp-10 elicits GnRH secretion through the required activation of phospholipase C, mobilization of intracellular Ca^{2+} and recruitment of ERK1/2 and p38 kinases (Castellano et al., 2006).

Studies from two different groups have analyzed the structure-activity relationships of Kp-10 (Niida et al., 2006; Orsini et al., 2007; Tomita et al., 2007a; Tomita et al., 2006; Tomita et al., 2007b; Tomita et al., 2008). These analyses indicate that the nature and the orientation of the side-chains of the five C-terminal residues are important for receptor binding and activation whereas the N-terminal amino acids are more tolerant to substitution by L-alanine or enantiomer residues (Niida et al., 2006; Orsini et al., 2007). In addition, in pursuing the development and analysis of new analogs for kisspeptin, one group has generated short-chain analogs, notably pentapeptides (Tomita et al., 2007a; Tomita et al., 2006; Tomita et al., 2007b; Tomita et al., 2008). To date, compound *p*FBz-Phe-Gly-Leu-Arg-Trp-NH_2 is the shortest kiss1r ligand that exhibits the same efficacy and potency as Kp-10 (Tomita et al., 2007b; Tomita et al., 2008). In SDS micelles, Kp-13 encompasses an α-helix from residues Asn^7 to Phe^{13} (Asn^4 and Phe^{10} in Kp-10, respectively) suggesting that the disruption of this α-helix could be responsible for the lower activity of inappropriately substituted compounds (Orsini et al., 2007).

Although these studies have provided valuable information regarding the individual contribution of each residue to kiss1r activation, there is still a lack of coordinate information on the potential activity of these modified kisspeptin compounds in a physiologically relevant target. Accordingly, in the present work, we have applied an interdisciplinary approach to attain an integrated analysis of the structure-activity relationships of a series of rat kp-10 analogs obtained by chemical substitution of each residue by alanine. To this end, we have evaluated the potential functional activity of

Molecular Pharmacology Fast Forward. Published on April 23, 2009 as DOI: 10.1124/mol.108.053751
This article has not been copyedited and formatted. The final version may differ from this version.

Ala-substituted kp-10 analogs using an *in vitro* assay model of kiss1r-transfected CHO-K1 cells, assessed the *in vivo* action of kp-10 and two analogs (selected from *in vitro* assays) on a well-characterized, physiologically relevant target for kisspeptins, *i.e.*, stimulation of luteinizing hormone (LH) release in rats, and finally studied the 3-D structure by molecular modeling under NMR restraints of these three selected compounds.

Material and methods

Chemicals and reagents for peptide synthesis

L-amino acid residues, the resins, O-benzotriazol-1-yl-*N,N,N',N'*-tetramethyluronium hexafluorophosphate (HBTU) and 1-hydroxy-benzotriazole (HOBt) were purchased from Applera-France (Courtaboeuf, France). Acetonitrile and *N*-methylpyrrolidin-2-one (NMP) were obtained from Carlo Erba (Val-de-Reuil, France). Diisopropylethylamine (DIEA), piperidine, trifluoroacetic acid (TFA) and other reagents were from Sigma-Aldrich (Saint-Quentin-Fallavier, France). Phospholipids dodecylphosphocholine-d_{38} (DPC-d_{38}, 99.1%) were from C/D/N isotopes (Pointe-Claire, Canada), D_2O and sodium 2,2-dimethyl-2-silapentane-5-sulphonate (DSS) were from Euriso-top (Gif-sur-Yvette, France).

Peptide synthesis

Rat metastin (rat kisspeptin-52; TSPCPPVENPTGHQRPPCATRSRLIPAPRGSVLVQ REKDMSAYNWNSFGLRY-NH_2), rat kp-10 (YNWNSFGLRY-NH_2), human Kp-10 (YNWNSFGLRF-NH_2) and L-alanine analogs of rat kp-10 (see Table 1) were synthesized (0.25 mmol scale for metastin; 0.1 mmol scale for all other peptides) on a Fmoc-PAL-PEG-PS resin for metastin and on a Rink amide 4-methylbenzhydrylamine resin for the other peptides using an Applied Biosystems model 433A automatic peptide synthesizer and the standard procedures, as previously described (Leprince et

Molecular Pharmacology Fast Forward. Published on April 23, 2009 as DOI: 10.1124/mol.108.053751
This article has not been copyedited and formatted. The final version may differ from this version.

al., 1998). All Fmoc-amino acids (1 mmol, 4 eq. or 10 eq.) were coupled by *in situ* activation with HBTU/HOBt (1.25 mmol:1.25 mmol, 5 eq. or 12.5 eq.) and DIEA (2.5 mmol, 10 eq. or 25 eq.) in NMP. Reactive side-chains were protected as follows: Arg, pentamethyldihydrobenzofuran (Pbf) sulfonylamide; Asn and Gln, trityl (Trt) amide; Ser, Thr and Tyr, tert-butyl (*t*Bu) ether; Asp and Glu, O-tert-butyl (O*t*Bu) ester; Cys, acetamidomethyl (Acm) thioether; His, trityl (Trt) amine; and Lys and Trp, tert-butyloxycarbonyl (Boc) carbamate. After completion of the chain assembly, cyclization of rat metastin was performed by $Tl(OCOCF_3)_3$ oxidation as previously described (Chatenet et al., 2006). Peptides were deprotected and cleaved from the resin by TFA as previously described (Chatenet et al., 2006; Leprince et al., 1998). Crude peptides were purified by reversed-phase HPLC (RP-HPLC) on a Vydac 218TP1022 C_{18} column (2.2 x 25 cm; Grace Discovery Sciences Alltech, Templemars, France) using a linear gradient (10-50% over 50 min) of acetonitrile/TFA (99.9:0.1, v/v) at a flow rate of 10 ml/min. Peptides were analyzed by RP-HPLC on a Vydac 218TP54 C_{18} column (0.46 x 25 cm; Grace Discovery Sciences Alltech) using a linear gradient (10-60% over 25 min) of acetonitrile/TFA at a flow rate of 1 ml/min. All peptides were characterized by MALDI-TOF mass spectrometry on a Voyager DE-PRO (Applera France) in the reflector mode with α-cyano-4-hydroxycinnamic acid as a matrix.

Cloning of the rat kiss1r, transfection and selection of monoclonal cell lines

Genomic DNA was extracted from rat pituitaries, using the Tripure Isolation Reagent (RocheMolecular Biochemicals, Mannheim, Germany) according to the manufacturer's protocol. The full length rat *kiss1r* was amplified by two PCR rounds, using a high-fidelity Taq polymerase (Ecozyme; Ecogen, Barcelona, Spain). For the first PCR round, specific primers were designed at the 5' and 3' regions of the coding sequence, respectively (sense, 5´ ATGGATATGGCG 3´; antisense, 5´ AGATACTGGTCTGG 3´), according to the known sequence of rat *kiss1r* (GenBank accession no. AF115516). The PCR product was subjected to a second amplification

Molecular Pharmacology Fast Forward. Published on April 23, 2009 as DOI: 10.1124/mol.108.053751
This article has not been copyedited and formatted. The final version may differ from this version.

using the same sense and antisense primers but including HindIII (upper, HindIII;5´ TACAAGCTTGCCATGGATATGGCG 3´) and EcoRI (lower, EcoRI;5´ TCAGGGAA TTCAGATACTGGTCTGG 3´) restriction sites. After the second PCR amplification, the rat *kiss1r* full-length cDNA was subcloned into the corresponding restriction sites of the pCDNA3.1 vector (Invitrogen, Barcelona, Spain). Identity of the cloned sequence was confirmed by sequencing at the Central Facilities of the University of Córdoba.

Chinese hamster ovary (CHO)-K1 cells were cultured to semiconfluence in 12-well plates using F12 medium supplemented with 10% fetal bovine serum and 1% antibiotic-antimycotic solution, and transfected with different concentrations of the recombinant plasmid, ranging from 3 to 5 µg, using Lipofectamine 2000 (Life Technologies, Inc., Barcelona, Spain). Twenty-four hours after transfection, media were replaced by fresh F12 containing 1 mg/ml of geneticin (G418; Life Technologies, Inc.). One week later, surviving cells were detached, diluted to 70 cells/ml and plated on 96-well plates at 0.7 cells/well. Monoclonal cell lines expressing rat *kiss1r* were followed daily by contrast phase microscopy. Seven independent monoclonal stable cell lines were obtained after a 3-week period of selection. By using quantitative RT-PCR, two cell lines were selected based on their expression levels being closest to physiological levels among all cell lines. Of these, one cell line was definitely selected based on its best performance in showing clear $[Ca^{2+}]_i$ responses to treatment with kp-10.

Measurement of free cytosolic calcium concentration ($[Ca^{2+}]_i$) using FlexStation technology

To compare the kiss1r agonistic activities of kisspeptin-52, kisspeptin-10 and Ala-substituted decapeptide analogs, the level of $[Ca^{2+}]_i$ following stimulation of CHO-K1 cells stably expressing *kiss1r* by these peptides was monitored by spectrofluorometry. The agonistic activity of each compound was assessed by calculating two distinct values: the percent activity (*i.e.* relative maximum agonistic

Molecular Pharmacology Fast Forward. Published on April 23, 2009 as DOI: 10.1124/mol.108.053751
This article has not been copyedited and formatted. The final version may differ from this version.

activity induced by each compound compared with the maximum signal induced by the addition of kp-10), and the EC_{50} value (*i.e.* the concentration required for 50% of the full agonistic activity induced by doses ranging from 10^{-12} to 10^{-5} M of each compound).

Functional assays were performed by first seeding 96-well black/clear microplates (Costar) with 40,000 cells/well 24 hours prior to assay. After overnight incubation at 37 ºC, cells were loaded for 1 h at 37 ºC with 4 mM Fluo-4 AM (Molecular Probes, Eugene, OR) in standard Hank's balanced salt solution buffer (Gibco, Carlsbad, CA) containing 5 mM HEPES (Sigma, Saint-Quentin-Fallavier, France) and 2.5 mM probenecid (Sigma). Cells were then washed 3x with standard Hank's balanced salt solution and changes in $[Ca^{2+}]_i$ induced by compound addition were measured using the FlexStation II system (Molecular Devices, Sunnyvale, CA) during the next 135 s. Responses were measured as peak fluorescent intensity minus basal fluorescent intensity at each concentration of agonist. Sigmoidal concentration-response curves were fitted with variable Hill slopes and EC_{50} values were generated using the Prism version 4.0 software (GraphPad Software, San Diego, CA).

Measurement of $[Ca^{2+}]_i$ in single cells

CHO-K1 cells stably transfected with rat *kiss1r* were incubated for 30 min at 37 °C with 2.5 mM of the Ca^{2+} indicator dye Fura-2 AM (Molecular Probes) in phenol red-free DMEM containing 20 mM Na_2HCO_3 (pH 7.4). Coverslips were washed with phenol red-free DMEM and mounted on the stage of a Nikon Eclipse TE2000-E microscope (Nikon, Tokyo, Japan) with attached back-thinned charge-coupled device cooled digital camera (ORCA II BT; Hamamatsu Photonics, Hamamatsu, Japan). Cells were examined under a 40X oil immersion objective during exposure to alternating 340- and 380-nm light beams, and the intensity of light emission at 505 nm was measured every 5 sec. Changes in $[Ca^{2+}]_i$ after administration of the compounds were recorded as background subtracted ratios of the corresponding excitation wavelengths (F340/F380) using the MetaFluor software (Imaging Corp., West Chester, PA).

Molecular Pharmacology Fast Forward. Published on April 23, 2009 as DOI: 10.1124/mol.108.053751
This article has not been copyedited and formatted. The final version may differ from this version.

In vivo *studies*

Adult Wistar male rats, bred in the Experimental Animal Department of the University of Córdoba, were used. The animals were maintained under constant conditions of light (14 h of light, from 7 AM) and temperature (22 °C), with free access to pelleted food and tap water. Procedures of intracerebroventricular (i.c.v.) administration of the testing compounds (kp-10 and/or Ala-substituted analogs) under conscious conditions were as previously described (Castellano et al., 2006; Navarro et al., 2004), following implantation (>24-48 h before pharmacological testing) of i.c.v. cannulae. To allow delivery of compounds into the lateral cerebral ventricle, the cannulae were lowered to a depth of 4 mm beneath the surface of the skull; the insert point was 1 mm posterior and 1.2 mm lateral to bregma. Correct positioning of the cannulae was visually inspected in the course of the experiments and confirmed post-mortem. Experimental procedures were approved by the Córdoba University Ethical Committee for animal experimentation and were conducted in accordance with the European Union normative for care and use of experimental animals.

In order to characterize the functionality of the selected kp-10 analogs *in vivo*, three different experiments were conducted. In *Experiment 1*, the effects on LH secretion of a single bolus of kp-10 or the Ala-substituted analogs were tested in intact male rats. To this end, groups of males (n = 10-12) received 10 µl i.c.v. injections of kp-10, [Ala^{6}]kp-10 or [Ala^{10}]kp-10 (dose: 1 nmol), and blood samples were taken by jugular veni-puncture at 0- (basal), 15-, 60- and 120-min after central administration. Animals i.c.v. injected with saline served as controls. In *Experiment 2*, the effects on LH secretion of the co-administration of each analog with kp-10 were explored in intact males. Thus, groups of male rats (n = 10-12) received 10 µl i.c.v. injections of 100 pmol kp-10 alone, or kp-10 together with 1 nmol doses of [Ala^{6}]kp-10 or [Ala^{10}]kp-10; rats i.c.v. injected with saline were used as controls. Blood samples for hormonal

Molecular Pharmacology Fast Forward. Published on April 23, 2009 as DOI: 10.1124/mol.108.053751
This article has not been copyedited and formatted. The final version may differ from this version.

determinations were taken by jugular veni-puncture at 0- (basal), 15-, 60- and 120-min after central administration. Finally, in *Experiment 3*, the effects of kp-10 analogs on pre-stimulated LH secretion were explored in orchidectomized (ORX) rats. Groups of male rats (n = 10-12) were subjected to bilateral ORX via the scrotal route as previously described (Navarro et al., 2004). One week after surgery, the animals received three consecutive i.c.v. injections (at 60-min intervals) of 1 nmol [Ala^{6}]kp-10 or 1 nmol [Ala^{10}]kp-10; rats receiving saline served as controls. Blood samples for hormonal determinations were taken by jugular veni-puncture at 15-min after each i.c.v. injection of the analogs.

Hormone measurements

Serum LH levels were measured in duplicate using a double-antibody radioimmunoassay method and reagents supplied by the NIH (Dr. AF Parlow, NIDDK National Hormone and Peptide Program; Torrance, CA). Rat LH-I-10 was labeled with ^{125}I using Iodo-Gen precoated tubes, following the instructions of the manufacturer (Pierce, Rockford, IL). Hormone concentrations were expressed using reference preparation LH-RP-3 as standard. The intra-assay coefficient of variation was <10% and the sensitivity of the assay was 3.75 pg/tube. All samples were measured in the same assay. Accuracy of hormone determinations was confirmed by assessment of rat serum samples of known hormone concentrations used as external controls.

NMR spectroscopy

Each peptide was dissolved at a concentration of 1.0 mM in 10% D_2O, 90% H_2O in the presence of 150 mM DPC-d_{38} for a micelle concentration of approximately 3 mM. DSS was added as an internal ^{1}H chemical shift reference.

All NMR experiments were performed on a Bruker Avance DMX 600 NMR spectrometer (Wissembourg, France) equipped with a triple resonance cryoprobe including shielded z-gradients. For all samples, 1D spectra were recorded at 5 K

intervals from 293 to 313 K. The following conventional two-dimensional experiments were carried out: 2D COSY, TOCSY and NOESY at 295 K and 308 K. NOESY spectra were collected at mixing times of 50, 80, 100, 150, 200 and 250 ms. TOCSY experiments were performed with a 80-ms MLEV-17 spin lock mixing pulse. During data acquisition, the water signal was suppressed by using the pulse-field gradient based watergate technique (Piotto et al., 1992) except for the COSY experiment where a low power presaturation was applied during the relaxation delay. TOCSY and NOESY experiments were performed in the phase-sensitive mode, using proportional phase incrementation method for quadrature detection (States-TPPI) (Marion D, 1989). Spectra were collected with 512 and 2048 complex data points in t_1 and t_2 dimensions. Data were processed on Silicon Graphics Indigo 2 XL or Windows workstations, using XWINNMR or TOPSPIN softwares (Bruker, Wissembourg, France). The f1 dimension was zero-filled to 1024 real data points. Time domain data were multiplied by shifted sinebell or gaussian functions in both dimensions prior to Fourier transformation. Proton chemical shifts were reported relative to DSS taken as an internal reference. The sequential assignment was performed at 308 K using the standard sequential assignment strategy (Wüthrich, 1986). $^{3}J_{HN\text{-}H\alpha}$ coupling constants were measured on 1D spectra.

Experimental NMR restraints

Distance restraints for structure calculations were derived from NOE cross-peaks in the NOESY spectrum recorded at 308 K with a mixing time of 150 ms. A NOESY spectrum recorded at 295 K allowed to solve some ambiguities due to overlapping of the resonance signals. NOE cross-peaks were integrated into distances by volume integration using the Felix software (Accelrys, Orsay, France). The NOE volumes were calibrated from well-resolved geminal H^{β} cross-peaks. The consistency of this calibration was verified on other geminal proton distances. A range of ±25% of the calculated distance was used to define the upper and lower bounds of the restraints

Molecular Pharmacology Fast Forward. Published on April 23, 2009 as DOI: 10.1124/mol.108.053751
This article has not been copyedited and formatted. The final version may differ from this version.

between H^N, H^α and H^β atoms. For other restraints, a range of ±12.5% of the squared calculated distance was used to take into account spin diffusion. Structure calculations were conducted with 65, 72, 93 unambiguous and 19, 15, 12 ambiguous distance restraints for kp-10, [Ala^6]kp-10 and [Ala^{10}]kp-10, respectively. ϕ dihedral angles were obtained from $^3J_{HN\text{-}H\alpha}$ coupling constants using the Karplus relation with the Pardi coefficients. For coupling constants with multiple solutions, the value was selected according to its consistency with secondary information provided by the NOE data.

Three-dimensional structure calculation

Three-dimensional structures were calculated *in vacuo* on a Silicon Graphics Indigo 2 XL station with the CNX program (Accelrys), using a random simulated annealing calculation. The target function was similar to that used by Nilges *et al.* and a force field adapted for NMR structure determination (parallhdg.pro and topallhdg.pro in X-PLOR) was used (Nilges et al., 1988). A first set of structures was generated, based on the amino acid sequence and on a starting set of distance restraints, using an *ab initio* simulated annealing protocol. During the whole process, the distance restraint force was kept to 50 kcal•$Å^{-2}$ and the NOE intensities were averaged with the "sum" option. Starting from an extended conformation, a first phase of 40 ps dynamics (timestep = 2 fs) at 1000 K was followed by 20 ps slow cooling step to 100 K (time step = 2 fs). A low weight of the van der Waals repulsive term was used at high temperature to allow a large conformation sampling. The variation of the slope of the asymptote in the NOE potential function allowed a progressive fit of the distance restraints. The structures leading to no systematic distance violation larger than 0.20 Å were submitted for further refinement. A 40-ps simulated annealing procedure from 1000 K to 100 K (timestep = 2 fs) with smoothing of the van der Waals repulsions and square-shapped NOE potential, was applied. A final minimization was carried out using the force field derived from CHARMM22 (files parallh22.pro and topallh22.pro) (Brooks BR, 1983) to yield a final set of optimized structures. Analysis of the structures made it possible to

Molecular Pharmacology Fast Forward. Published on April 23, 2009 as DOI: 10.1124/mol.108.053751
This article has not been copyedited and formatted. The final version may differ from this version.

resolve ambiguities in the assignment of NOE cross-peaks, which arose from chemical shift degeneracy. This procedure was iterated several times by calculating, at each step, a new set of structures with an improved list of restraints. Nevertheless, some ambiguous assignments still remained and were introduced with an appropriate treatment in CNX (Nilges M, 1995). A final set of structures was then generated. The final structures were analyzed by CNX and displayed by using SYBYL (Tripos, Saint Louis, MO) and MOLSCRIPT (Kraulis PJ, 1991).

Statistical analysis

Hormonal determinations were conducted in duplicate; data are presented as mean ± SEM of at least 10 independent determinations per group. When appropriate, integrated LH secretory responses following i.c.v. administration of the testing compounds were calculated as the area under the curve (AUC), following the trapezoidal rule. Functional experiments were performed at least in triplicate and data, expressed as mean ± S.E.M, were analyzed with the Prism software (Graphpad Software). The EC_{50} from the concentration-response curve values were determined using a sigmoidal dose-response fit with variable slope. Statistical comparisons of hormonal values, as well as potencies of kp-10 and kp-10 analogs were analyzed by ANOVA followed by a Dunnett's multiple comparison test or a Student-Newman-Keuls multiple range test. Differences were considered significant when $P<0.05$

Results

Earlier studies have shown that the C-terminal decapeptide of human Kisspeptin (45-54; Kp-10) exhibits higher receptor affinity and evokes more potent functional responses than its extended counterparts (Ohtaki et al., 2001). To further explore the structural requirements of this core sequence, we have carried out Ala-scan of rat kp-10 to identify important residues for kiss1r-agonistic activity. To this aim,

Molecular Pharmacology Fast Forward. Published on April 23, 2009 as DOI: 10.1124/mol.108.053751
This article has not been copyedited and formatted. The final version may differ from this version.

we synthesized rat metastin, rat and human Kp-10 and ten rat kp-10 Ala-analogs (Table 1) by standard Fmoc-based solid phase peptide synthesis, and we tested their functional activity *in vitro* on r*kiss1r* -transfected CHO-K1 cells and, for selected compounds, on their ability to elicit LH responses *in vivo*.

Peptide analysis

RP-HPLC analysis of rat metastin, rat and human Kp-10 and Ala-substituted rat kp-10 revealed that the purity of all peptides was higher than 99% (Table 1). For all peptides, the molecular weight observed by MS analysis was consistent with the theoretical value (Table 1).

In vitro *functional assay for kisspeptins and synthetic substituted analogs*

Activities of the peptides were determined based on the kinetics of $[Ca^{2+}]_i$ in CHO-K1 cells stably transfected with r*kiss1r*, by using a multi-mode FlexStation system. As shown in Fig 1A and Table 2, kp-10 analogs generated by Ala point substitutions of amino acid residues 1 to 5 and 7 to 9, displayed EC_{50} values ranging from 1.04×10^{-8} to 1.27×10^{-7} M, which closely resemble those found for rat and human Kp-10 (EC_{50} = 1.54 - 2.6 x 10^{-8} M), suggesting that amino acids located at those positions are not critical for kp-10 functional activity, and possibly, for its binding to kiss1r. In clear contrast, [Ala^6]kp-10 and [Ala^{10}]kp-10 showed an increased EC_{50} value (> 6.46 μM), well above that found for kp-10 and the other analogs studied (Fig 1B & Table 2).

Based on the above data, we performed specific assays to test the potential antagonistic activity of the [Ala^6]kp-10 and [Ala^{10}]kp-10 analogs. The data showed that only the [Ala^6]kp-10 analog had an apparent antagonistic property, with an IC_{50} value of 9.31×10^{-7} M (Fig 1C & Table 2), which would reflect a potential competitive action. However, a Schild analysis of the data obtained in these *in vitro* assays evidenced that

Molecular Pharmacology Fast Forward. Published on April 23, 2009 as DOI: 10.1124/mol.108.053751
This article has not been copyedited and formatted. The final version may differ from this version.

[Ala^6]kp-10 did not behave as a typical competitive reversible antagonist (data not shown).

To further understand the properties of the Ala-substituted kisspeptin analogs, we examined their actions on the dynamics of $[Ca^{2+}]_i$ in individual CHO-K1 cells stably expressing r*kiss1r*. In line with the studies on cell populations, administration of kisspeptin analogs substituted in position 1 to 5 and 7 to 9 did not result in appreciable changes in response as compared to those caused by rat kp-10 and rat metastin (Fig. 2A). Conversely, treatments with [Ala^6]kp-10 and [Ala^{10}]kp-10 showed a significant decrease in the proportion of responsive cells which was accompanied by a marked increase in the time required by responsive cells to reach maximal amplitude of response (Fig. 2B).

Taken together, the results obtained *in vitro* indicate that position 6 and 10 are critical for kiss1r activation and thus possibly for kiss1r binding.

***Effects of kp-10 and Ala-substituted analogs on LH secretion* in vivo**

In vivo studies monitored the ability of [Ala^6]kp-10 and [Ala^{10}]kp-10 to mimic or antagonize the effects of rat kp-10 in terms of dynamic LH secretion. First, analysis of LH responses to administration of a single bolus of kp-10 or the substituted analogs revealed that Ala^6 substitution resulted in a significant reduction in the LH-releasing effects of the compound; yet, [Ala^6]kp-10 retained its capacity to stimulate LH secretion. Thus, while kp-10 evoked an 8-fold increase in serum LH levels that persisted up to 120-min after i.c.v. administration, an equimolar dose of [Ala^6]kp-10 induced a 4-fold increase of circulating LH only at 15-min after injection. In good agreement, integrated (120-min) LH responses to [Ala^6]kp-10 were ~20% of those elicited by kp-10. In contrast, Ala^{10} substitution fully prevented the ability of the compound to induce LH secretion following i.c.v. administration, with individual and integrated LH responses which were strictly similar to those observed in vehicle-injected controls (Fig. 3).

Molecular Pharmacology Fast Forward. Published on April 23, 2009 as DOI: 10.1124/mol.108.053751
This article has not been copyedited and formatted. The final version may differ from this version.

The effects of the combined administration of kp-10 and each of the above analogs were also tested *in vivo*. In order to underscore potential antagonistic effects of the Ala-substituted peptides, and considering the enormous potency of kp-10 in inducing LH release after i.c.v. administration (Navarro et al., 2005), 1 nmol doses of the analogs were centrally co-administered with sub-maximal 100 pmol doses of kp-10. As shown in Figure 4, i.c.v. injection of 100 pmol kp-10 elicited robust LH secretory responses that peaked at 15-min and progressively decreased thereafter, in keeping with previous reports (Navarro et al., 2005). Similar secretory profiles were observed after i.c.v. co-injection of kp-10 and [Ala^{6}]kp-10 or [Ala^{10}]kp-10, with individual time-point responses that were analogous to those elicited by the administration of kp-10 alone. In good agreement, integrated (120-min) LH responses following i.c.v. injection of kp-10 were similar regardless of the co-administration of [Ala^{6}]kp-10 or [Ala^{10}]kp-10 (Fig. 4).

Finally, the effects of selected Ala-substituted kp-10 analogs on stimulated LH secretion were also assayed in ORX rats. Of note, ORX has been proven to induce a state of increased expression of *kiss1* in the hypothalamus that seems mechanistically relevant for the elevation of circulating LH levels (Smith et al., 2005). Thus, it was predicted that central blockade of kisspeptins should bring about a detectable reduction of circulating LH in ORX animals. Protocols of repeated i.c.v. injection of 1 nmol boluses of [Ala^{6}]kp-10 or [Ala^{10}]kp-10, with a total of 3 injections at 60-min intervals, were implemented, and serum LH levels were monitored 15-min after each injection. As expected, one-week ORX resulted in the elevation of basal LH levels over control values in intact male rats (10.5 ± 0.9 ng/ml in ORX vs. 0.8 ± 0.16 ng/ml). Repeated i.c.v. administration of 1 nmol [Ala^{6}]kp-10 evoked further increases in circulating LH levels at 15-min after each injection of the compound. In contrast, central injection of [Ala^{10}]kp-10 failed to modify the pre-elevated LH levels, at any of the time-points studied (Fig. 5).

Molecular Pharmacology Fast Forward. Published on April 23, 2009 as DOI: 10.1124/mol.108.053751
This article has not been copyedited and formatted. The final version may differ from this version.

NMR solution structure of rat kp-10, [Ala^6]kp-10 and [Ala^{10}]kp-10

The three-dimensional structures of kp-10, [Ala^6]kp-10 and [Ala^{10}]kp-10 were calculated by a simulated annealing protocol using NMR restraints collected on the 150-ms NOESY spectra recorded at 308 K.

For kp-10, among the 100 generated structures, 88 structures were consistent with the experimental data and the standard covalent geometry. The structures presented no distance violation larger than 0.2 Å and no ideal geometry violations. Analysis of the ϕ/ψ angles (data not shown) revealed a good convergence for residues Asn^4 to Tyr^{10}. These residues were found in the ϕ/ψ space energetically allowed and were located in the right–handed helix region of the Ramachandran plot (data not shown). In this region, all kp-10 structures exhibited a similar helical backbone folding, as shown by the superimposition of the 88 structures (Figure 6A, <rmsd> = 0.36 Å). The ϕ/ψ values obtained for Asn^4-Tyr^{10} residues were intermediate between the characteristic values of the α- and 3_{10} helix types. Consistent with these observations, both $HN_{i+4} \rightarrow CO_i$ and $HN_{i+3} \rightarrow CO_i$ hydrogen bonds, typical of α- and 3_{10}-helix, respectively, were observed in most of the structures.

For [Ala^6]kp-10 and [Ala^{10}]kp-10, 77 and 81 structures, respectively, were retained among the 100 generated structures. As for kp-10, these structures were consistent with the experimental data and the standard covalent geometry, with no distance violation larger than 0.2 Å and no ideal geometry violations. They exhibited a well-defined helicoidal folding for residues Trp^3-Tyr^{10} in [Ala^6]kp-10 structures (Figure 6B, <rmsd> = 0.41 Å) and for residues Asn^4-Leu^8 in [Ala^{10}]kp-10 structures (Figure 6C, <rmsd> = 0.38 Å).

For [Ala^6]kp-10, analysis of the ϕ/ψ angles and hydrogen bonds revealed α-helical characteristics for residues Trp^3, Asn^4, Leu^8 and Arg^9, and 3_{10}-helical characteristics for residues Ser^5, Arg^6 and Tyr^{10}. Although Gly^7 was found in the right-

Molecular Pharmacology Fast Forward. Published on April 23, 2009 as DOI: 10.1124/mol.108.053751
This article has not been copyedited and formatted. The final version may differ from this version.

handed helix region of the Ramachandran plot, it could not be classified in any canonical helicoidal type.

For [Ala^{10}]kp-10, as for kp-10, ϕ/ψ angles and hydrogen bonds of residues Asn^{4}-Leu^{8} presented mixed characteristics of α- and 3_{10} helices. The two last residues, Arg^{9} and Ala^{10}, did not exhibit any helicoidal folding.

Discussion

Structure-activity relationship studies constitute a valuable approach to obtain critical information in the development of novel analogs of biologically active peptides with potential clinical applications. The strength of this type of studies is greatly enhanced by applying a combined, interdisciplinary approach, where structural analysis and *in vitro* activity assays of the compounds under investigation are complemented with *in vivo* functional testing of selected compounds. In the present work, an Ala-scan of rat kp-10 was performed to determine the essential structural requirements for kiss1r agonistic activity.

Our two-pronged *in vitro* approach to assess the functional features of the Ala-substituted analogs revealed that the Phe^{6} and Tyr^{10} residues of kp-10 are critical for its kiss1r-agonistic activity. Indeed, when examined both in whole cell populations by using a FlexStation system and at the single cell level, amino acids 6 and 10 appeared as key functional residues for kp-10. The essential role of the C-terminal residue was expected, since previous studies have shown the indispensable role of this amino acid to maintain an appropriate function not only of kisspeptin (Niida et al., 2006; Ohtaki et al., 2001; Orsini et al., 2007) but also of other members of the RF-amide family of peptides, which includes prolactin-releasing peptide and neuropeptide FF, where the C-terminal Arg-Phe is also critical for their biological activity (Boyle et al., 2005; Mazarguil et al., 2001). However, the native C-terminal phenylalanine residue can be

replaced by different aromatic moieties, such as tyrosine, tryptophan, substituted-phenylalanine or naphtylalanine, without significant loss of potency or efficacy of RFamide peptides (Boyle et al., 2005; Mazarguil et al., 2001; Tomita et al., 2006). Conversely, replacement of the C-terminal phenylalanine by saturated-side-chain residues such as cyclohexylalanine suppresses the biological activity of kp-10 (Orsini et al., 2007). In the case of neuropeptide FF, the distance of the aromatic ring from the peptide backbone seems to be crucial for access to the binding pocket since homophenylalanine and phenylglycine moieties markedly reduce the affinity of the peptide for its cognate receptor (Mazarguil et al., 2001).

The present results extend and complement previous studies that have analyzed the pharmacological and functional features of Ala-substituted analogs for human Kp-10 and Kp13 (Niida et al., 2006; Orsini et al., 2007), by applying a similar approach to that used herein. *In vitro* testing of human Kp-10 showed that residues Phe^{6}, Leu^{8}, Arg^{9} and Phe^{10} are crucial to the activity of the peptide (Niida et al., 2006; Orsini et al., 2007). Consistent with these data, we found that Phe^{6} and Tyr^{10} in rat kp-10 are also critical for *r*kiss1r activation. Conversely, in our study Leu^{8} and Arg^{9} do not seem to be playing such a key role. Based on the above, [Ala^{6}]kp-10 and [Ala^{10}]kp-10 analogs were selected for integral analysis, including assessment of their effects in terms of LH secretion *in vivo* and comparison of their 3D-structure under NMR restraints.

In vivo tests on the LH-releasing capacities of [Ala^{6}]kp-10 and [Ala^{10}]kp-10 compounds confirmed our initial observations *in vitro* on the essential roles of Phe^{6} and Tyr^{10} for full agonistic activity of kisspeptins at the kiss1r level. However, such *in vivo* analyses unveiled also interesting differences in the functional relevance of these two residues. Thus, Phe^{6} in rat kp-10 appears critical for maximal activation of kiss1r *in vivo* but, perhaps, dispensable for receptor binding, as [Ala^{6}]kp-10 was still able to evoke significant LH secretory responses, albeit of lower magnitude than those of kp-10. This

Molecular Pharmacology Fast Forward. Published on April 23, 2009 as DOI: 10.1124/mol.108.053751
This article has not been copyedited and formatted. The final version may differ from this version.

suggests its function as partial agonist. In keeping with this view, even in a ten-fold excess, [Ala^6]kp-10 was unable to inhibit the stimulatory effect of exogenous kp-10, neither was it able to suppress the stimulated LH levels in a model of sustained elevation of the prevailing kisspeptin tone, such as the ORX rat (Navarro et al., 2004). Thus, in contrast to that suggested by the results obtained *in vitro* on rkiss1r-CHO cells, we did not find comparable evidence to support that [Ala^6]kp-10 might operate as antagonist of kisspeptin actions *in vivo*.

Our *in vivo* work also confirmed that Ala^{10} substituted kp-10 is completely devoid of detectable activity *in vivo* as (i) it did not induce LH release per se, (ii) it did not prevent the effects of kp-10 on LH secretion, and (iii) it did not affect pre-elevated LH levels in ORX rats after its repeated administration. Given the conspicuous lack of agonistic or antagonistic activity of [Ala^{10}]kp-10, it is proposed that such C-terminal position could be essential for kisspeptin binding to kiss1r; a possibility that needs to be experimentally confirmed. From a more general stand-point, our results emphasize the importance of an integral characterization of kisspeptin derivatives, involving *in vivo* testing. In this context, it is noticeable that previously developed pentapeptides, with apparent full agonistic activity at kiss1r in cellular models, have not been evaluated in terms of gonadotropin secretion *in vivo*. Studies on pentapeptides derived from C-terminal kisspeptin have been mainly focused on the discovery and/or design of analogs with superagonistic properties, which could be used to profit the antimetastatic abilities of kisspeptin (metastin). However, in the field of reproductive endocrinology, the functional potency and efficacy of kp-10 is already remarkable in *in vivo* studies, and this lends difficult the discovery and/or design of superagonistic kisspeptin analogs. On the other hand, in this particular field, it would be highly valuable to obtain compounds with antagonistic capacity for the kisspeptin/kiss1r system, as this pair seems to play a key, hierarchically relevant role in the control of the reproductive axis.

Molecular Pharmacology Fast Forward. Published on April 23, 2009 as DOI: 10.1124/mol.108.053751
This article has not been copyedited and formatted. The final version may differ from this version.

The conformations of kp-10, [Ala^6]kp-10 and [Ala^{10}]kp-10 were investigated by ^{1}H-NMR spectroscopy and restrained molecular dynamics in a DPC-water mixture, a membrane-mimetic medium. The structure of rat kp-10 encompasses a helix spanning from Asn^4 to Tyr^{10}, with mixed α and 3_{10} characteristics, preceded by a disordered N-terminal region. Recently, the solution structure of human Kp-13 has been determined in a SDS-water mixture, another membrane mimetic medium (Orsini et al., 2007). Human Kp-13 differs from rat kp-10 by an N-terminal extension (Leu-Pro-Asn) and the substitution of the C-terminal residue (Phe-NH_2 instead of Tyr-NH_2). Interestingly, the helical structure of human Kp-13 runs from Asn^7 to Phe^{13} *i.e.* at the same relative position as in rat kp-10, but the type of helix in human Kp-13 had not been determined (Orsini et al., 2007). The observation that human Kp-13 and rat kp-10 share a common helical domain, together with the fact that both peptides behave as full kiss1r agonists (Kotani et al., 2001; Muir et al., 2001; Ohtaki et al., 2001) strongly suggests that the helical structure plays a relevant role in kiss1r binding and/or activation.

Substitution of native Phe^6 by an Ala moiety slightly modified the helical structure of the peptide. Specifically, the helix was extended by one residue in its N-terminal region (Trp^3-Tyr^{10}), and the Gly^7 moiety did not show canonical helical characteristics. These findings suggest that Ala^6 substitution did not dramatically impair the helical conformation of the peptide but only weakly modified the local arrangement around the alanine residue. This mild perturbation is compatible with the partial agonistic profile of [Ala^6]kp-10.

Substitution of native Tyr^{10} residue by an Ala moiety provoked a marked destabilization of the helical structure in the C-terminal part of the peptide. While a helix with similar characteristics to those of kp-10 was observed between the Asn^4 and Leu^8 residues, no structuration was detected for the last two C-terminal residues, Arg^9 and Ala^{10}. Since, [Ala^{10}]kp-10 was totally devoid of agonistic and antagonistic properties, it

Molecular Pharmacology Fast Forward. Published on April 23, 2009 as DOI: 10.1124/mol.108.053751
This article has not been copyedited and formatted. The final version may differ from this version.

appears that the shortening of the C-terminal helix may be responsible, at least in part, for the lack of activity of the peptide, as already suggested (Orsini et al., 2007).

In summary, our data demonstrate that the replacement of the Tyr^{10}-NH_2 residue of kp-10 by an L-Ala-NH_2 moiety abolishes the agonistic activity of this peptide at kiss1r both *in vitro* and *in vitro*, whereas the replacement of the Phe^6 residue by L-Ala yields a weak antagonist *in vitro* which shows severely reduced agonistic activity *in vivo*. The altered activities of the [Ala^{10}]kp-10 and [Ala^6]kp-10 analogs are attributable to complete destabilization of the C-terminal region of the helix, and to a moderate distortion of the helical structure around position 6, respectively. These data, coupled to the type of experimental strategy used herein to examine structure-activity relationships pave the way for the future design and characterization of new kiss1r agonists and/or antagonists with potential experimental and clinical applications.

Molecular Pharmacology Fast Forward. Published on April 23, 2009 as DOI: 10.1124/mol.108.053751
This article has not been copyedited and formatted. The final version may differ from this version.

References

Boyle RG, Downham R, Ganguly T, Humphries J, Smith J and Travers S (2005) Structure-activity studies on prolactin-releasing peptide (PrRP). Analogues of PrRP-(19-31)-peptide. *J Pept Sci* **11**:161-165.

Brooks BR, Bruccoleri RE, Olafson BD, States DJ, Swaminathan S, Karplus M. (1983) CHARMM: a program for macromolecular energy minimization and dynamics calculations. *J Comput Chem* **4**:187-217.

Castaño JP, Martinez-Fuentes AJ, Gutierrez-Pascual E, Vaudry H, Tena-Sempere M and Malagon MM (2009) Intracellular signaling pathways activated by kisspeptins through GPR54: Do multiple signals underlie function diversity? *Peptides* **30**:10-15.

Castellano JM, Navarro VM, Fernandez-Fernandez R, Castaño JP, Malagon MM, Aguilar E, Dieguez C, Magni P, Pinilla L and Tena-Sempere M (2006) Ontogeny and mechanisms of action for the stimulatory effect of kisspeptin on gonadotropin-releasing hormone system of the rat. *Mol Cell Endocrinol* **257-258**:75-83.

Chatenet D, Dubessy C, Boularan C, Scalbert E, Pfeiffer B, Renard P, Lihrmann I, Pacaud P, Tonon MC, Vaudry H and Leprince J (2006) Structure-activity relationships of a novel series of urotensin II analogues: identification of a urotensin II antagonist. *J Med Chem* **49**:7234-7238.

d'Anglemont de Tassigny X, Fagg LA, Dixon JP, Day K, Leitch HG, Hendrick AG, Zahn D, Franceschini I, Caraty A, Carlton MB, Aparicio SA and Colledge WH (2007) Hypogonadotropic hypogonadism in mice lacking a functional Kiss1 gene. *Proc Natl Acad Sci USA* **104**:10714-10719.

de Roux N, Genin E, Carel JC, Matsuda F, Chaussain JL and Milgrom E (2003) Hypogonadotropic hypogonadism due to loss of function of the KiSS1-derived peptide receptor GPR54. *Proc Natl Acad Sci USA* **100**:10972-10976.

Funes S, Hedrick JA, Vassileva G, Markowitz L, Abbondanzo S, Golovko A, Yang S, Monsma FJ and Gustafson EL (2003) The KiSS-1 receptor GPR54 is essential for the development of the murine reproductive system. *Biochem Biophys Res Commun* **312**:1357-1363.

Kotani M, Detheux M, Vandenbogaerde A, Communi D, Vanderwinden JM, Le Poul E, Brezillon S, Tyldesley R, Suarez-Huerta N, Vandeput F, Blanpain C, Schiffmann SN, Vassart G and Parmentier M (2001) The metastasis suppressor gene KiSS-1 encodes kisspeptins, the natural ligands of the orphan G protein-coupled receptor GPR54. *J Biol Chem* **276**:34631-34636.

Kraulis PJ (1991) MOLSCRIPT: a program to produce both detailed and schematic plots of protein structures. *J Appl Cryst* **24**:946-950.

Lapatto R, Pallais JC, Zhang D, Chan YM, Mahan A, Cerrato F, Le WW, Hoffman GE and Seminara SB (2007) Kiss1-/- mice exhibit more variable hypogonadism than Gpr54-/- mice. *Endocrinology* **148**:4927-4936.

Lee JH, Miele ME, Hicks DJ, Phillips KK, Trent JM, Weissman BE and Welch DR (1996) KiSS-1, a novel human malignant melanoma metastasis-suppressor gene. *J Natl Cancer Inst* **88**:1731-1737.

Lee JH and Welch DR (1997) Suppression of metastasis in human breast carcinoma MDA-MB-435 cells after transfection with the metastasis suppressor gene, KiSS-1. *Cancer Res* **57**:2384-2387.

Leprince J, Gandolfo P, Thoumas JL, Patte C, Fauchere JL, Vaudry H and Tonon MC (1998) Structure-activity relationships of a series of analogues of the octadecaneuropeptide ODN on calcium mobilization in rat astrocytes. *J Med Chem* **41**:4433-4438.

Marion D, Ikura M, Tschudin R, Bax A. (1989) Rapid recording of 2D NMR spectra without phase cycling. Application to the study of hydrogen exchange in proteins. *J Magn Reson* **85**:393-399.

Mazarguil H, Gouarderes C, Tafani JA, Marcus D, Kotani M, Mollereau C, Roumy M and Zajac JM (2001) Structure-activity relationships of neuropeptide FF: role of C-terminal regions. *Peptides* **22**:1471-1478.

Mead EJ, Maguire JJ, Kuc RE and Davenport AP (2007) Kisspeptins: a multifunctional peptide system with a role in reproduction, cancer and the cardiovascular system. *Br J Pharmacol* **151**:1143-1153.

Muir AI, Chamberlain L, Elshourbagy NA, Michalovich D, Moore DJ, Calamari A, Szekeres PG, Sarau HM, Chambers JK, Murdock P, Steplewski K, Shabon U, Miller JE, Middleton SE, Darker JG, Larminie CG, Wilson S, Bergsma DJ, Emson P, Faull R, Philpott KL and Harrison DC (2001) AXOR12, a novel human G protein-coupled receptor, activated by the peptide KiSS-1. *J Biol Chem* **276**:28969-28975.

Nash KT and Welch DR (2006) The KISS1 metastasis suppressor: mechanistic insights and clinical utility. *Front Biosci* **11**:647-659.

Navarro VM, Castellano JM, Fernandez-Fernandez R, Barreiro ML, Roa J, Sanchez-Criado JE, Aguilar E, Dieguez C, Pinilla L and Tena-Sempere M (2004) Developmental and hormonally regulated messenger ribonucleic acid expression of KiSS-1 and its putative receptor, GPR54, in rat hypothalamus and potent luteinizing hormone-releasing activity of KiSS-1 peptide. *Endocrinology* **145**:4565-4574.

Navarro VM, Castellano JM, Fernandez-Fernandez R, Tovar S, Roa J, Mayen A, Nogueiras R, Vazquez MJ, Barreiro ML, Magni P, Aguilar E, Dieguez C, Pinilla L and Tena-Sempere M (2005) Characterization of the potent luteinizing hormone-releasing activity of KiSS-1 peptide, the natural ligand of GPR54. *Endocrinology* **146**:156-163.

Niida A, Wang Z, Tomita K, Oishi S, Tamamura H, Otaka A, Navenot JM, Broach JR, Peiper SC and Fujii N (2006) Design and synthesis of downsized metastin (45-54) analogs with maintenance of high GPR54 agonistic activity. *Bioorg Med Chem Lett* **16**:134-137.

Nilges M (1995) Calculation of protein structures with ambiguous distance restraints. Automated assignment of ambiguous NOE crosspeaks and disulphide connectivities. *J Mol Bio* **245**:645-660.

Nilges M, Gronenborn AM, Brunger AT and Clore GM (1988) Determination of three-dimensional structures of proteins by simulated annealing with interproton distance restraints. Application to crambin, potato carboxypeptidase inhibitor and barley serine proteinase inhibitor 2. *Protein Eng* **2**:27-38.

Ohtaki T, Shintani Y, Honda S, Matsumoto H, Hori A, Kanehashi K, Terao Y, Kumano S, Takatsu Y, Masuda Y, Ishibashi Y, Watanabe T, Asada M, Yamada T, Suenaga M, Kitada C, Usuki S, Kurokawa T, Onda H, Nishimura O and Fujino M (2001) Metastasis suppressor gene KiSS-1 encodes peptide ligand of a G-protein-coupled receptor. *Nature* **411**:613-617.

Orsini MJ, Klein MA, Beavers MP, Connolly PJ, Middleton SA and Mayo KH (2007) Metastin (KiSS-1) mimetics identified from peptide structure-activity relationship-derived pharmacophores and directed small molecule database screening. *J Med Chem* **50**:462-471.

Piotto M, Saudek V and Sklenar V (1992) Gradient-tailored excitation for single-quantum NMR spectroscopy of aqueous solutions. *J Biomol NMR* **2**:661-665.

Popa SM, Clifton DK and Steiner RA (2008) The role of kisspeptins and GPR54 in the neuroendocrine regulation of reproduction. *Annu Rev Physiol* **70**:213-238.

Roa J, Aguilar E, Dieguez C, Pinilla L and Tena-Sempere M (2008) New frontiers in kisspeptin/GPR54 physiology as fundamental gatekeepers of reproductive function. *Front Neuroendocrinol* **29**:48-69.

Roa J and Tena-Sempere M (2007) KiSS-1 system and reproduction: comparative aspects and roles in the control of female gonadotropic axis in mammals. *Gen Comp Endocrinol* **153**:132-140.

Seminara SB, Messager S, Chatzidaki EE, Thresher RR, Acierno JS, Jr., Shagoury JK, Bo-Abbas Y, Kuohung W, Schwinof KM, Hendrick AG, Zahn D, Dixon J, Kaiser UB, Slaugenhaupt SA, Gusella JF, O'Rahilly S, Carlton MB, Crowley WF, Aparicio SA and Colledge WH (2003) The GPR54 gene as a regulator of puberty. *New Engl J Med* **349**:1614-1627.

Smith JT, Dungan HM, Stoll EA, Gottsch ML, Braun RE, Eacker SM, Clifton DK and Steiner RA (2005) Differential regulation of KiSS-1 mRNA expression by sex steroids in the brain of the male mouse. *Endocrinology* **146**:2976-2984.

Tomita K, Narumi T, Niida A, Oishi S, Ohno H and Fujii N (2007a) Fmoc-based solid-phase synthesis of GPR54-agonistic pentapeptide derivatives containing alkene- and fluoroalkene-dipeptide isosteres. *Biopolymers* **88**:272-278.

Tomita K, Niida A, Oishi S, Ohno H, Cluzeau J, Navenot JM, Wang ZX, Peiper SC and Fujii N (2006) Structure-activity relationship study on small peptidic GPR54 agonists. *Bioorc Med Chem* **14**:7595-7603.

Tomita K, Oishi S, Cluzeau J, Ohno H, Navenot JM, Wang ZX, Peiper SC, Akamatsu M and Fujii N (2007b) SAR and QSAR studies on the N-terminally acylated pentapeptide agonists for GPR54. *J Med Chem* **50**:3222-3228.

Tomita K, Oishi S, Ohno H and Fujii N (2008) Structure-activity relationship study and NMR analysis of fluorobenzoyl pentapeptide GPR54 agonists. *Biopolymers* **90**:503-511.

Wüthrich K (1986) *NMR of Proteins and Nucleics Aids.*, New York.

Molecular Pharmacology Fast Forward. Published on April 23, 2009 as DOI: 10.1124/mol.108.053751
This article has not been copyedited and formatted. The final version may differ from this version.

FOOTNOTES

Support: This work was supported by grants from Junta de Andalucía (BIO-0139, BIO-310 and CTS-1705), Ministerio de Ciencia e Innovación/FEDER (BFU2004-03883, BFU2007-60180/BFI and BFU2008-00984/BFI), Instituto de Salud Carlos III – Ministerio de Sanidad y Consumo (PI042082), Spain, French National Research Agency (ANR, project FrenchKiSS ANR-07-BLAN-0056-04), the Institut Fédératif de Recherches Multidisciplinaires sur les Peptides (IFRMP 23), the Plate-forme Régionale de Recherche en Imagerie Cellulaire de Haute-Normandie (PRIMACEN), Inserm (U413) and the Région Haute-Normandie.

Molecular Pharmacology Fast Forward. Published on April 23, 2009 as DOI: 10.1124/mol.108.053751
This article has not been copyedited and formatted. The final version may differ from this version.

Legend to figures

Figure 1. *In vitro* evaluation of the functional properties of rat kp-10 and Ala-substituted analogs of kp-10. Effects of increasing concentrations of the different kisspeptins were assessed by using FlexStation technology to measure the levels of free cytosolic Ca^{2+} concentration ($[Ca^{2+}]_i$) on cultured CHO-K1 cells stably transfected with kiss1r. **A.** Average dose-response curves for $[Ca^{2+}]_i$ observed for [Ala^1]-, [Ala^2]-, [Ala^3]-, [Ala^4]-, [Ala^5]-, [Ala^7]-, [Ala^8]- and [Ala^9]kp-10. **B.** Average dose-response curves for $[Ca^{2+}]_i$ for [Ala^6]- and [Ala^{10}]kp-10. **C.** Competition assay of [Ala^6]kp-10 and [Ala^{10}]kp-10. Increasing doses of Ala-susbstituted analog were applied in presence of a fixed concentration of rat kp-10 and changes in $[Ca^{2+}]_i$ levels were measured. Values represent the mean ± SEM from at least three independent experiments.

Figure 2. *In vitro* analysis of the functional features of rat metastin (rat kp-52), rat kp-10, and kp-10 analogs on single cells. Microfluorimetry was applied to determine the effects of treatment with metastin, kp-10 and Ala-substituted analogs of kp-10 on the levels of $[Ca^{2+}]_i$ in single CHO-K1 cells stably transfected with kiss1r. **A.** Percentage of cells that was responsive to a challenge with 10^{-6} M of the corresponding kisspeptin. **B.** Time required by responsive cells to reach maximal level of $[Ca^{2+}]_i$ after application of the corresponding kisspeptin (10^{-6} M). Values represent the mean ± SEM of a minimum of n=3 independent experiments, and within each experiment a minimum of 80 individual cells were measured.

Figure 3. *In vivo* analysis of the effects of Ala^6 and Ala^{10} kp-10 analogs on LH secretion in adult male rats. The experimental animals were injected i.c.v. with a single dose of 1 nmol of [Ala^6]kp-10, [Ala^{10}]kp-10 or kp-10, and blood samples for LH determination were obtained before (0-min) and at 15-, 60-min and 120-min after compound administration. Rats i.c.v. injected with vehicle served as controls. In addition to the time-course profiles (*left panel*), integrated secretory responses to central administration of kp-10 analogs (calculated as AUC over the 120-min study-period) are

also shown in the *right panel*. Hormonal values are the mean ± S.E.M. of at least 10 independent determinations per group. ** $p<0.01$ vs. corresponding vehicle-injected group; **a** $p<0.01$ vs. corresponding kp-10 injected group (ANOVA followed by Student-Newman-Keuls multiple range test).

Figure 4. *In vivo* analysis of the effects of co-administration of kp-10 and Ala^6 or Ala^{10} analogs on LH secretion in adult male rats. The experimental animals were injected i.c.v. with a 100 pmol dose of kp-10, alone or in combination with a 1 nmol bolus of [Ala^6]kp-10 or [Ala^{10}]kp-10 or kp-10. Blood samples for LH determination were obtained before (0-min) and at 15-, 60-min and 120-min after compound administration. Rats i.c.v. injected with vehicle served as controls. In addition to the time-course profiles (*left panel*), integrated secretory responses to central administration of kp-10 analogs (calculated as AUC over the 120-min study-period) are also shown in the *right panel*. Hormonal values are the mean ± S.E.M. of at least 10 independent determinations per group. ** $p<0.01$ vs. corresponding vehicle-injected group (ANOVA followed by Student-Newman-Keuls multiple range test).

Figure 5. *In vivo* analysis of the effects of Ala^6 and Ala^{10} kp-10 analogs on LH hyper-secretion in orchidectomized (ORX) rats. One week after ORX, the animals received three consecutive i.c.v. injections (at 60-min intervals) of 1 nmol [Ala^6]kp-10 or 1 nmol [Ala^{10}]kp-10, and blood samples for LH determinations were taken by jugular veni-puncture at 15-min after each i.c.v. injection of the analogs. ORX rats i.c.v. injected with vehicle served as controls. Hormonal values are the mean ± S.E.M. of at least 10 independent determinations per group. ** $p<0.01$ vs. corresponding vehicle-injected group (ANOVA followed by Student-Newman-Keuls multiple range test).

Figure 6. Backbone (N, Cα, C' atoms) superimposition of the lowest conformers of (A) kp-10 between residues Asn^4-Tyr^{10}, (B) [Ala^6]kp-10 between residues Trp^3-Tyr^{10}, and (C) [Ala^{10}]kp-10 between residues Asn^4-Leu^8.

Molecular Pharmacology Fast Forward. Published on April 23, 2009 as DOI: 10.1124/mol.108.053751
This article has not been copyedited and formatted. The final version may differ from this version.

Table 1 – Analytical data for compounds **1**-**13**

Compound number	Peptide	HPLC		MS	
		R*t* (min)[a]	Purity (%)	Calcd[b]	Obsd[c]
1	rat metastin	20.35	99.95	5833.91	5833.12[d]
2	*r*Kp-10	19.35	99.07	1318.62	1318.54
3	*h*kp-10	20.64	99.83	1302.63	1302.80
4	[Ala^{1}]kp-10	18.37	99.99	1226.60	1226.52
5	[Ala^{2}]kp-10	19.43	99.66	1275.62	1275.65
6	[Ala^{3}]kp-10	16.40	99.96	1203.58	1203.63
7	[Ala^{4}]kp-10	19.84	99.89	1275.62	1275.54
8	[Ala^{5}]kp-10	19.62	99.80	1302.63	1302.54
9	[Ala^{6}]kp-10	16.62	99.70	1242.59	1242.68
10	[Ala^{7}]kp-10	19.33	99.99	1332.64	1332.79
11	[Ala^{8}]kp-10	17.92	99.78	1276.58	1276.38
12	[Ala^{9}]kp-10	19.97	99.62	1233.56	1233.25
13	[Ala^{10}]kp-10	17.77	99.85	1226.60	1226.43

[a]Retention time determined by RP-HPLC. [b]Theoretical monoisotopic MH^+ value. [c]m/z value (MH^+) assessed by MALDI-TOF in the reflector mode. [d]m/z value (MH^+) assessed by MALDI-TOF in the linear mode.

Molecular Pharmacology Fast Forward. Published on April 23, 2009 as DOI: 10.1124/mol.108.053751
This article has not been copyedited and formatted. The final version may differ from this version.

Table 2 – Functional parameters of the response of kiss1r-CHO-K1 cells to treatment with different kisspeptins as measured using FlexStation technology

Peptide	Agonist			Antagonist		
	n	Max. Efficacy (%)[a]	EC_{50}	n	Max.Efficacy (%)	IC_{50}
*r*kp-10	11	100	1.5E-08 ± 5.3E-09			
*h*Kp-10	4	100.3 ± 7.3	2.6E-08 ± 8.8E-09			
[Ala^{1}]kp-10	6	87.2 ± 2.3	1.7E-08 ± 4.8E-09			
[Ala^{2}]kp-10	6	91.2 ± 5.4	1.4E-0 8 ± 2.8E-09			
[Ala^{3}]kp-10	5	92.2 ± 5.5	1.0E-08± 5.2E-09			
[Ala^{4}]kp-10	5	89.6 ± 5.6	7.3E-08± 1.7E-09			
[Ala^{5}]kp-10	4	79.0 ± 2.8	1.6E-08± 1.6E-09			
[Ala^{6}]kp-10	7	49.9 ± 2.8	6.5E-06± 3.0E-06	10		9.3E-07± 1.0E-07
[Ala^{7}]kp-10	4	88.9 ± 3.7	3.4E-08± 1.4E-08			
[Ala^{8}]kp-10	5	84.1 ± 5.5	1.0E-07± 6.3E-08			
[Ala^{9}]kp-10	6	74.2 ± 4.2	1.7E-07± 4.9E-08			
[Ala^{10}]kp-10	4	24.1 ± 5.6	--	10	Inactive	--

a The maximum efficacy is expressed as a percentage of the amplitude induced by 10^{-6} M rkp-10

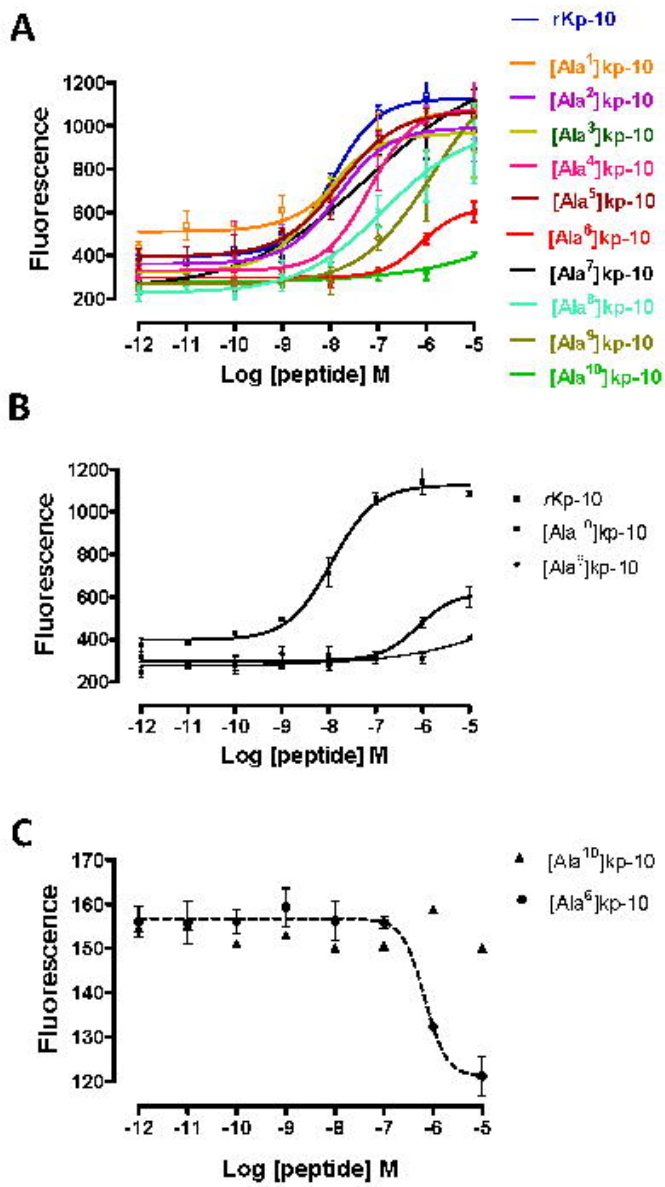
A
rKp-10
[Ala1]kp-10
[Ala2]kp-10
[Ala3]kp-10
[Ala4]kp-10
[Ala5]kp-10
[Ala6]kp-10
[Ala7]kp-10
[Ala8]kp-10
[Ala9]kp-10
[Ala10]kp-10
Fluorescence
1200
1000
800
600
400
200
-12 -11 -10 -9 -8 -7 -6 -5
Log [peptide] M
B
rKp-10
[Ala n]kp-10
[Ala]kp-10
Fluorescence
1200
1000
800
600
400
200
-12 -11 -10 -9 -8 -7 -6 -5
Log [peptide] M
C
[Ala10]kp-10
[Ala6]kp-10
Fluorescence
170
160
150
140
130
120
-12 -11 -10 -9 -8 -7 -6 -5
Log [peptide] M

Figure 1

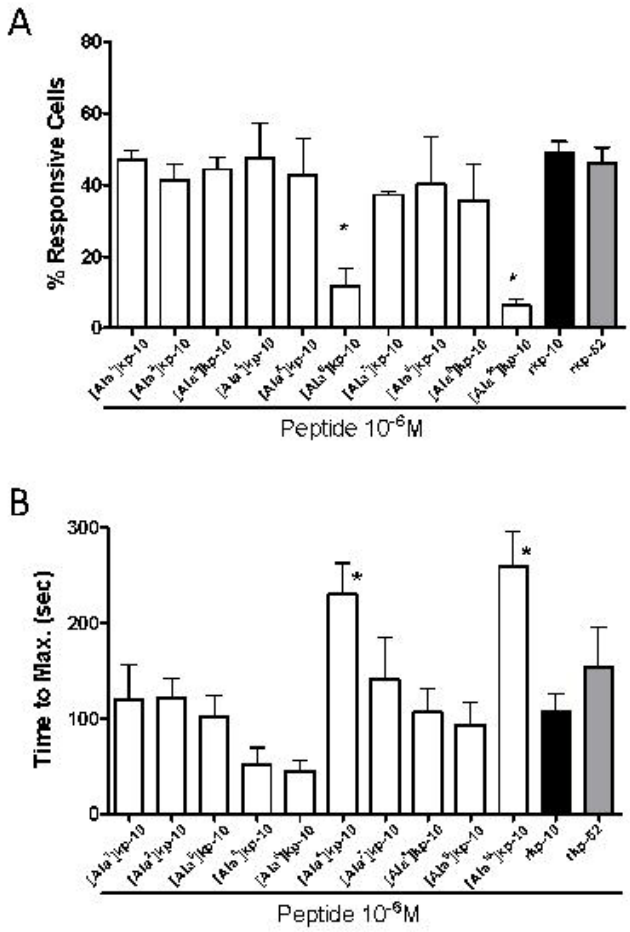
A
% Responsive Cells
80
60
40
20
0
*
*
[Ala 1]rp-10
[Ala 2]rp-10
[Ala 3]rp-10
[Ala 4]rp-10
[Ala 5]rp-10
[Ala 6]rp-10
[Ala 7]rp-10
[Ala 8]rp-10
[Ala 9]rp-10
[Ala 10]rp-10
rrp-10
rrp-52
Peptide 10-6M
B
Time to Max. (sec)
300
200
100
0
*
*
[Ala 1]rp-10
[Ala 2]rp-10
[Ala 3]rp-10
[Ala 4]rp-10
[Ala 5]rp-10
[Ala 6]rp-10
[Ala 7]rp-10
[Ala 8]rp-10
[Ala 9]rp-10
[Ala 10]rp-10
rhp-10
rhp-52
Peptide 10-6M

Figure 2

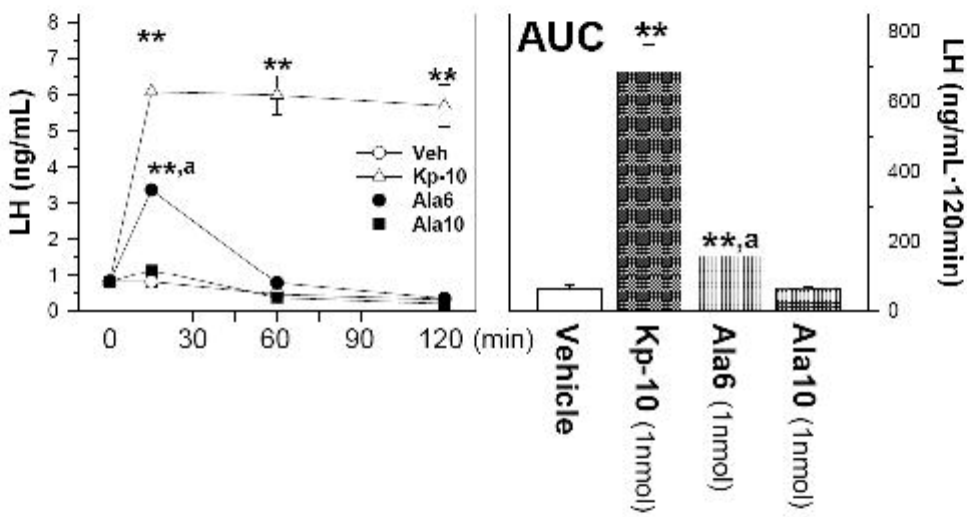
LH (ng/mL)
8
7
6
5
4
3
2
1
0
**
**
**
**,a
Veh
Kp-10
Ala6
Ala10
0
30
60
90
120 (min)
AUC
**
**,a
800
600
400
200
0
LH (ng/mL·120min)
Vehicle
Kp-10 (1nmol)
Ala6 (1nmol)
Ala10 (1nmol)

Figure 3

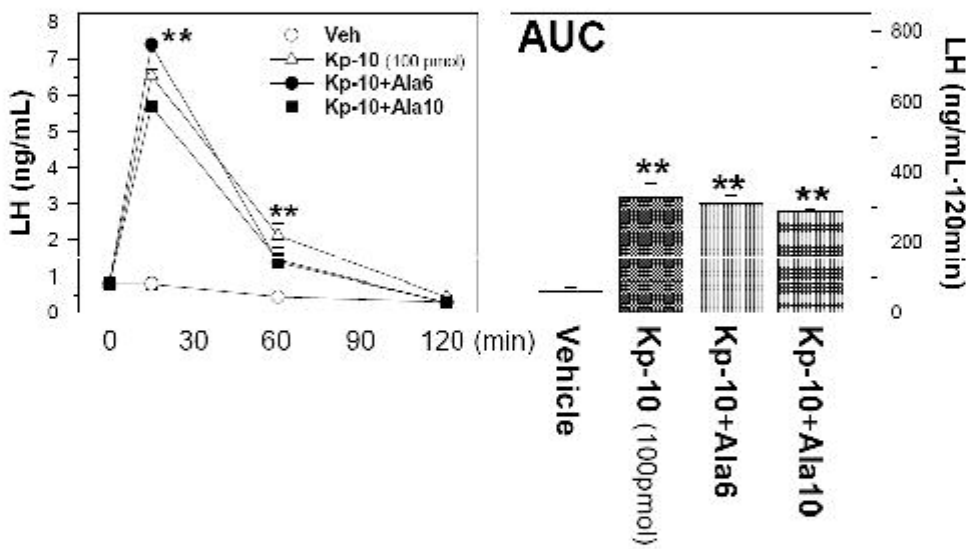
LH (ng/mL)
0
1
2
3
4
5
6
7
8
0
30
60
90
120 (min)
**
**
Veh
Kp-10 (100 pmol)
Kp-10+Ala6
Kp-10+Ala10
AUC
LH (ng/mL·120min)
0
200
400
600
800
**
**
**
Vehicle
Kp-10 (100pmol)
Kp-10+Ala6
Kp-10+Ala10

Figure 4

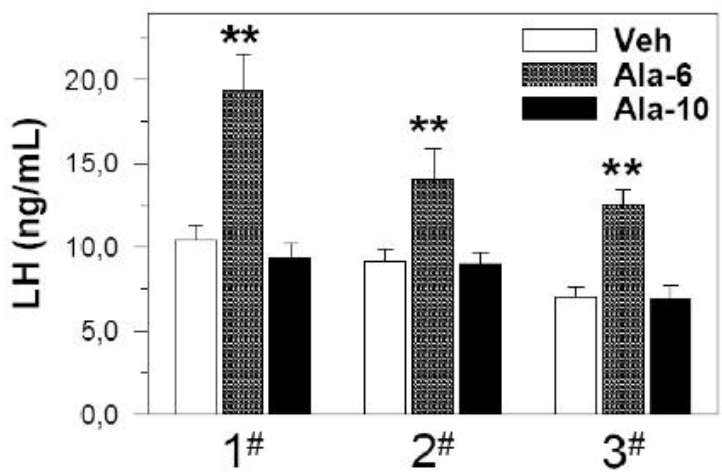

Figure 5

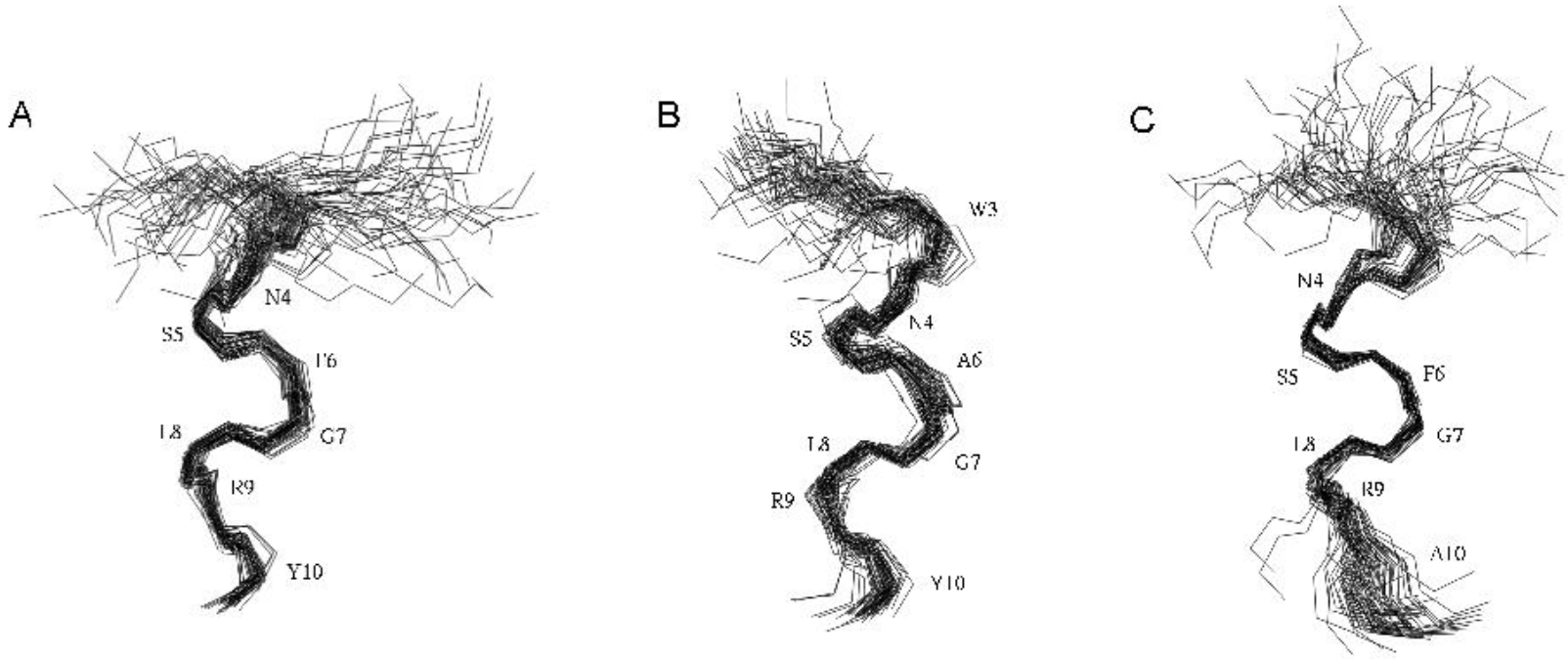
A
N4
S5
T6
T8
G7
R9
Y10
B
W3
N4
S5
A6
T8
G7
R9
Y10
C
N4
S5
F6
T8
G7
R9
A10

Figure 6